https://doi.org/10.24867/GRID-2026-p91

A Case Study in Functionally Graded Lattice Design for a Surfskate Deck: Workflow and Reduced-Scale Prototype

ABSTRACT

Skateboard and surfskate decks are typically built from multi-ply laminates whose stiffness is largely uniform across the board, regardless of how load is distributed in use. This case study explores an alternative: a single deck whose internal lattice varies in strut thickness and cell layout according to a local load-intensity field. Using Grasshopper for Rhinoceros 3D, a parametric deck is generated, the field is thresholded into four bands (rigid core, transition, compliant mid-span, edge), and each band is populated with a strut lattice and meshed volumetrically (OpenVDB) for fused filament fabrication (FFF). In this first prototype the field is an analytic proxy based on distance to the truck mounts, not a finite element result; coupling to Karamba3D shell analysis is the immediate next step. The workflow is demonstrated on a 240 mm reduced-scale PLA deck that follows the longitudinal camber and includes strut-free zones at the truck-mount positions, generated by suppressing struts locally rather than by a post-hoc Boolean cut. Hand loading showed the rigid core held as intended, while the thinnest struts in the compliant and edge bands fractured rather than flexed, indicating PLA is unsuitable for this strut geometry at this scale. The aim is to show, through one concrete example, that load-informed lattice grading is a feasible route to digitally fabricated, single-piece sports equipment, and to document the pipeline and its current simplifications as groundwork for a more general design method.

Panagiota Ligka [1]
Athina Tziarou [1]
Renata Gudaitiene [2]
Panagiotis Kyratsis [1]

[1] Department of Product and Systems Design Engineering, University of Western Macedonia, Koila, Western Macedonia
[2] Kaunas Kolegija, Higher Education Institution, Kaunas, Lithuania

KEY WORDS
Case study, functionally graded lattices, generative design, additive manufacturing, sports equipment design

1. Introduction

Skateboard decks are conventionally made from glued wood plies, and their stiffness is set by ply count, thickness and orientation, and is largely uniform across the surface (Willard & Loferski, 2018). Deck flex is nonetheless a recognised selection criterion among riders: stiffer boards are associated with responsive “pop” and precision, while more compliant boards are associated with comfort, damping and smooth carving. Surfskates, which use pivoting truck systems to emulate surfing-style turns, make carving response a primary design concern. Because a laminate cannot readily place stiffness where it is needed, designers must largely accept one compromise for the whole board. Additive manufacturing relaxes this constraint. Functionally graded lattices allow relative density and cell geometry to change continuously or in steps within a single printed part, and grading driven by load fields builds on established ideas in structural optimisation and cellular solids (Bendsøe & Kikuchi, 1988; Gibson & Ashby, 1997; Li et al., 2020).

This paper describes such a workflow, built in GrasshopperTM for Rhinoceros 3DTM, and a first reduced-scale prototype printed by FFF in PLA, building on a generative design methodology previously applied to different applications (Ligka, Manavis & Kyratsis, 2026; Manavis et al., 2022). The aims are: (i) to define a parametric deck and truck-mount layout; (ii) to convert a load-intensity field into discrete lattice bands; (iii) to

generate a graded lattice for each band suitable for FFF; and (iv) to compare the printed deck's hand-tested flex qualitatively with the grading pattern. The work is intentionally scoped as a proof of pipeline, and its simplifications are stated in Sections 2.2, 2.3 and 4.

2. Methods

2.1. Parametric deck and truck-mount zones

The deck outline is a closed planar curve with rounded nose and tail, defined by length and width sliders, and lofted to a longitudinally cambered surface (centre raised relative to the nose and tail). A signed camber parameter also permits a rocker profile (centre dropped) at negative values; the prototype uses positive camber only. A quad-dominant analysis mesh is generated whose target edge length sets the lattice cell pitch. Two elliptical zones mark the truck mounting areas along the longitudinal axis. Their centres are placed 15% of deck length from each end (a wheelbase of 0.70 L). The layout is symmetric about the deck centre by design, for this proof of pipeline: (i) it removes setback as a free variable, so band behaviour can be attributed to the grading rather than the layout; (ii) with a symmetric outline and camber, the proxy field should yield a near mirror-symmetric band partition, which serves as a built-in sanity check; and (iii) it matches the symmetric (twin-tip) outline used. Asymmetric truck setback is left for later work, together with the asymmetric pop and carve load cases, which will break this symmetry in the final field.

The full-scale deck is 800 mm long. The prototype is a 0.30-scale version (240 mm) to fit the printer's build volume. Outline and camber are scaled uniformly, while cell pitch (4.5 mm) and shell thickness (5 mm) are set independently of scale so that the lattice does not collapse into a solid. A full-scale version of the same definition was also generated and mesh-validated per band (Section 4).

2.2. Load-intensity field and banding

In the present prototype the load-intensity field is an analytic proxy computed per mesh face from a linear decay with distance to the truck zones, combined with a camber falloff term. It is not the output of a finite element solve. The proxy allowed the banding-to-lattice pipeline to be developed and validated independently of the structural solver. The camber falloff term was implemented but not tested independently, so its influence on the band pattern was not evaluated.

The intended field is the per-face envelope (maximum) of principal von Mises stress from two Karamba3D shell load cases: a tail "pop" load and an offset "carve" load with vertical and lateral components, with pinned supports at the truck zones (Preisinger, 2013). A torsional couple is a planned extension (Section 4).

Table 1
Band definitions and lattice parameters (default thresholds)

Band	Normalized intensity	Lattice type	Strut diameter (mm)
Rigid core	> 0.75	Cubic-type edge lattice	2.5
Transition	0.50- 0.75	Same topology, thinner struts	~1.3
Compliant mid-span	0.25- 0.50	Diagonal edge-strut lattice	~1.0
Edge	< 0.25	Diagonal edge-strut lattice, thinnest struts	0.9

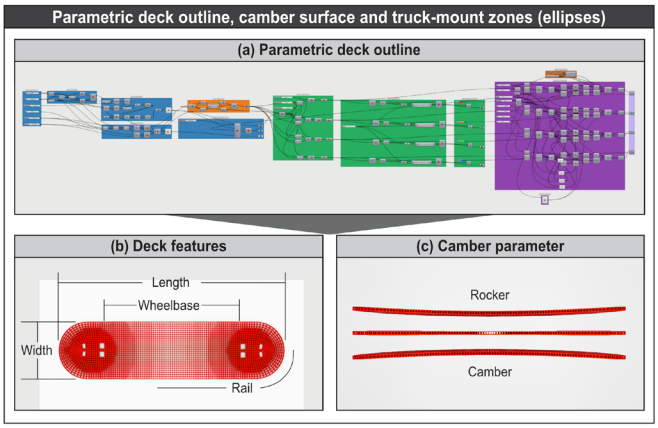
2.3. Lattice generation

Each band mesh is duplicated into a bottom layer and a top layer, offset along the surface normal by the shell thickness (measured between outer faces) and joined by vertical struts at welded vertices. Both layers follow the camber of the deck surface in Section 2.1 rather than a flat reference plane. In the rigid-core and transition bands, struts follow the edges of the analysis mesh to form a cubic-type edge lattice. In the two lower bands, diagonal struts spanning across each quad face are used instead. Cell pitch is absolute (4.5 mm) and scale-independent by construction: the upstream remesh edge length is divided by the scale factor so the final printed cell size stays 4.5 mm regardless of scale.

Struts are converted to volumetric distance fields and meshed per band with the Dendro plugin (an OpenVDB wrapper, version 1.3) (Museth, 2013), which yields watertight iso-surface meshes. The voxel size was 0.3 mm. Dendro requires strut radius to sufficiently exceed the voxel size for reliable iso-surface extraction; for the thinnest struts (0.9 mm diameter, 0.45 mm radius) against a 0.3 mm voxel size, the radius-to-voxel ratio was 1.5.

The four bands are meshed independently and exported as four separate watertight bodies that meet at shared boundary curves, rather than as a single unified shell (~5.2 million total faces across bands, validated in Rhino). Attempts at a mesh Boolean union of the full strut network were unreliable and were abandoned.

The version of Dendro used has no native unit-cell library, so re-entrant auxetic cells could not be generated directly. The two lower bands instead use diagonal struts at low diameter. This is a placeholder



» **Figure 1:** *Parametric deck outline, camber surface and truck-mount zones (ellipses)*

for future re-entrant auxetic cells and is not expected to exhibit a negative Poisson's ratio; no such behaviour is claimed or measured for this prototype.

Eight strut-free zones at the truck-mount positions (four per truck, matching a representative bolt pattern scaled with the deck) are left open in the rigid-core band by suppressing strut generation locally rather than by a subtractive Boolean cut on the finished mesh. This is implemented as a toggleable filter, so the same definition can generate an uninterrupted rigid-core lattice when mounting provision is not required.

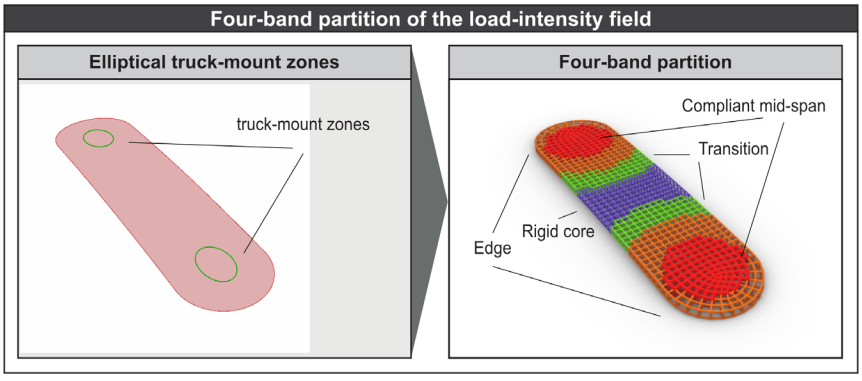
2.4. Fabrication

The deck was printed on a Bambu Lab P2S with a 0.4 mm nozzle in Bambu Basic PLA. Layer height was set to 0.2 mm with 3 outer perimeter walls, a print speed of 60 mm/s, and a nozzle temperature of 215°C using Bambu Studio with standard tree supports. The four band bodies were printed together as a single multi-body job, with boundaries meeting at shared contact curves rather than overlapping. The minimum printable strut diameter was 0.8 mm, twice the nozzle diameter; the thinnest band used (0.9 mm) sits above this floor with margin. PLA was chosen for its low cost and fast, reliable printing, which suited rapid iteration on a proof-of-pipeline prototype. At 0.30 scale the prototype is a demonstrator of the workflow and is not intended for riding.

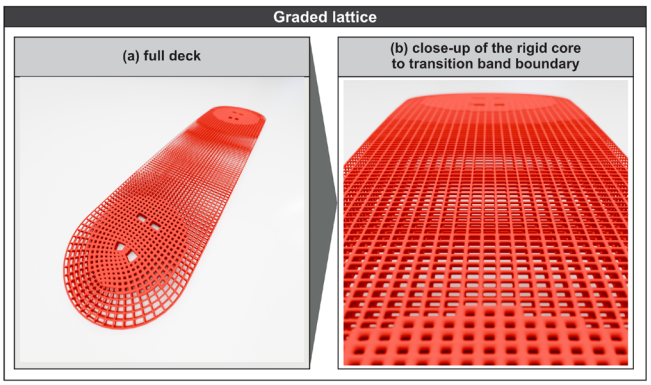
3. Results

3.1. Deck geometry and band partition

Figure 1 shows the parametric deck with its truck-zone ellipses, and Figure 2 the four-band partition of the analysis mesh. The rigid core forms two zones centred on the truck mounts, and the transition band wraps these and extends toward the rails. The compliant mid-span band lies between the two truck zones, and the edge band occupies the nose, tail and rail perimeter. This arrangement follows from the construction of the proxy field, which places the highest intensity around the truck zones, and should not be read as validation of the grading.



» **Figure 2:** *Four-band partition of the load-intensity field (rigid core, transition, compliant mid-span, edge)*



» **Figure 3:** *Graded lattice: (a) full deck; (b) close-up of the rigid core to transition band boundary. Strut diameter decreases from the rigid core to the transition band, though the step is subtle at this render scale and lighting; bands are not colour-coded in this figure (cf. Figure 2)*

3.2. Lattice output

Figure 3 shows the generated lattice, and Table 2 lists the prototype parameters. Each of the four bands was meshed as a separate watertight body, approximately 5.2 million faces in total across all four components, and all four pass mesh validation in Rhino (closed, manifold, no degenerate faces) after the repair step in Section 2.3.

Table 2
Prototype parameters

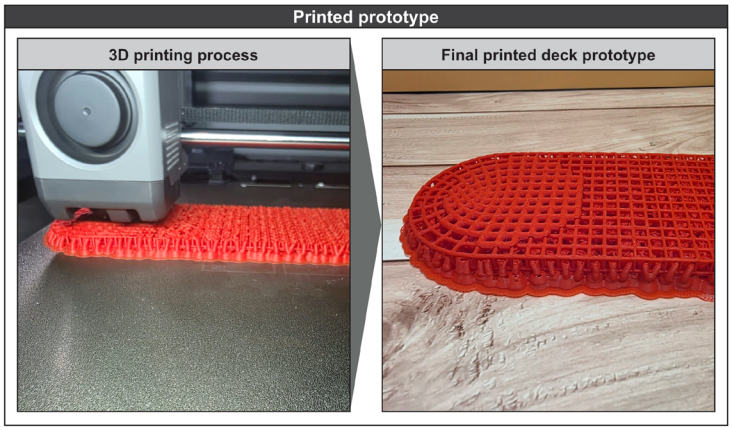
Parameter	Value
Deck length (scaled)	240 mm (0.30 × 800 mm)
Cell pitch	4.5 mm
Shell thickness	5.0 mm
Strut diameter	0.9 mm (minimum) to 2.5 mm (Table 1)
Voxel size	0.3 mm
Band thresholds	0.25, 0.50, 0.75
Material / printer	PLA / Bambu Lab P2S, 0.4 mm nozzle

3.3. Printed prototype and flex behavior

During hand-loading and support removal, several of the thinnest (edge-band, 0.9 mm) struts fractured rather than flexed; PLA's low strain-to-failure made it unsuitable for the sub-1 mm compliant struts, which required elastic bending rather than brittle fracture to behave as intended. This indicates that material choice, not only strut geometry, is a binding constraint on the graded-lattice concept: a flexible printable material (e.g. a TPU) is likely necessary for the compliant and edge bands to function as designed, while a stiffer material such as PLA may remain appropriate for the rigid core.

4. Discussion

The workflow shows that a load-intensity field can be carried through banding, lattice construction and volumetric meshing into a printable, parametric definition. The main value at this stage is the pipeline itself: every dimension, threshold and strut diameter remains a live parameter, so a redesign means regenerating the defini-



» **Figure 4:** *Printed prototype (left: in progress on the build plate; right: completed part before load testing). Several edge-band struts subsequently fractured under hand loading; see Section 3.3*

tion rather than remodelling the deck. The most important findings for later versions were practical: lattice cell pitch must be decoupled from deck scale, struts must be sized against voxel size for reliable meshing, and mesh Boolean operations on the full strut network proved unreliable at this density. A volumetric union of the band fields in Dendro, rather than a mesh-level Boolean, is the route we intend to test for a single unified shell.

The following limitations should be read alongside any result:

- Load field. The banding is driven by an analytic proxy, not FEA, so the pattern is a hypothesis about where stiffness is needed. With supports at the truck zones, the largest bending moment from a rider's weight lies between them, so the compliant mid-span runs against simple beam intuition and needs to be checked against a solved field. The camber falloff term was also not tested independently.
- Banding. Bands are stepped, and the default thresholds (0.25, 0.50, 0.75) were not optimised or compared with alternatives. Continuous grading is planned.
- Loading. Real deep carving involves asymmetric weight transfer and torsion along the long axis. The planned carve load case includes only vertical and lateral components, with a torsional couple as future work.
- Geometry. Two features of real decks are omitted from the base surface: transverse concave (the side-to-side dish across the width, used by riders for foot location and leverage) and nose and tail kicks (the upturned ends, which contribute to pop and control). Longitudinal camber is present and is followed by the lattice shell. The truck layout is also symmetric, and asymmetric setback is left for later work. All of these should be added in later versions.
- No auxetic behaviour. The compliant bands use diagonal struts as a placeholder, not a re-entrant or chiral topology. No claim of negative Poisson's ratio or indentation resistance is made for this prototype. True auxetic cells need a strut-based generator with native re-entrant unit cells, or a custom cell definition, and would require direct mechanical characterisation to confirm (Kolken & Zadpoor, 2017).
- Band assembly. The four lattice bands are exported as separate watertight bodies meeting at shared boundaries rather than as a single unified shell. A mesh Boolean union was attempted but proved unreliable at this strut density and was not pursued further.
- Scale, material and fabrication. The deck is printed at 0.30 scale in PLA, a stiff, brittle polymer with limited elastic recovery; its absolute stiffness, damping and pop are not representative of a conventional laminated deck or a rideable board. The full print job took 9 h 20 min using Bambu Studio's automatic tree supports. Several of the thinnest (0.9 mm) edge-band struts fractured during hand loading and support removal rather than flexing elastically, confirming that PLA's low strain-to-failure is unsuitable for this strut geometry; support strategy and orientation for thin-strut bands also warrant evaluation in future prints. A flexible filament such as TPU is the immediate next material to test for the compliant and edge bands, while a stiffer material such as PLA may remain appropriate for the rigid core. A full-scale (800 mm) version of the same definition was generated and mesh-validated per band, but required multi-part segmentation to fit the build volume and was not fabricated for this paper.
- Testing. Manual deflection testing is qualitative. It had no uniform-lattice control and no measured load or displacement, so it cannot separate the effect of grading from that of geometry and supports. It is no substitute for instrumented stiffness measurements or rider trials.
- Rider relevance. The grading, with stiffness at the truck zones where load is transferred and flex elsewhere, is intended to reflect how riders discuss deck flex. Testing with riders, and comparison with commercial surfskate decks, would be needed to show that the graded layout produces a ride that skaters actually prefer.



» **Figure 5:** *Illustrative concept render (not a functional test) showing the intended in-use context of a full-scale, assembled version of the design*

Figure 5 illustrates the intended full-scale application as a non-functional concept render; the prototype reported here was not ridden.

5. Conclusions

The parametric Grasshopper workflow maps a load-intensity field to four lattice bands and produces an FFF-ready, camber-following graded lattice

deck with toggleable strut-free zones at the truck mounts, demonstrated as a 0.30-scale (240 mm) PLA prototype. Hand loading showed that the rigid core remained stiff as intended, but the thinnest struts in the compliant and edge bands fractured under load rather than flexing, indicating that PLA is not a suitable material for this strut geometry at this scale.

6. Acknowledgments

The authors acknowledge the support of the University of Western Macedonia and Polis University in facilitating this research.

7. References

Bendsøe, M.P. and Kikuchi, N. (1988) 'Generating optimal topologies in structural design using a homogenization method', *Computer Methods in Applied Mechanics and Engineering*, 71(2), pp. 197–224. DOI: 10.1016/0045-7825(88)90086-2

Gibson, L.J. and Ashby, M.F. (1997) *Cellular Solids: Structure and Properties*. 2nd ed. Cambridge: Cambridge University Press. DOI: 10.1017/CBO9781139878326

Kolken, H.M.A. and Zadpoor, A.A. (2017) 'Auxetic mechanical metamaterials', *RSC Advances*, 7(9), pp. 5111–5129. DOI: 10.1039/c6ra27333e

Li, Y., Feng, Z., Hao, L., Huang, L., Xin, C., Wang, Y., Bilotti, E., Essa, K., Zhang, H., Li, Z., Yan, F. and Peijs, T. (2020) 'A Review on Functionally Graded Materials and Structures via Additive Manufacturing: From Multi-Scale Design to Versatile Functional Properties', *Advanced Materials Technologies*, 5. DOI: 10.1002/admt.201900981

Ligka, P., Manavis, A. and Kyratsis, P. (2026) 'Design of a lampshade using generative design methodology', *Computer-Aided Design & Applications*, 24(2), pp. 119–132. DOI: 10.14733/cadaps.2027.119-132

Manavis, A., Firtikiadis, L., Spahiu, T., Efkolidis, N. and Kyratsis, P. (2022) 'Parametric Architectural Design using shapes and structures', *Journal of Graphic Engineering and Design*, 13(4), pp. 13–20. DOI: 10.24867/JGED-2022-4-013

Museth, K. (2013) 'VDB: High-resolution sparse volumes with dynamic topology', *ACM Transactions on Graphics*, 32(3), Article 27. DOI: 10.1145/2487228.2487235

Preisinger, C. (2013) 'Linking structure and parametric geometry', *Architectural Design*, 83(2), pp. 110–113. DOI: 10.1002/ad.1564

Willard, D.T. and Loferski, J.R. (2018) 'Skateboards as a Sustainable Recyclable Material', *Recycling*, 3(4), Article 20. DOI: 10.3390/recycling3020020



© 2026 Authors. Published by the University of Novi Sad, Faculty of Technical Sciences, Department of Graphic Engineering and Design. This article is an open access article distributed under the terms and conditions of the Creative Commons Attribution license 4.0 Serbia (http://creativecommons.org/licenses/by/4.0/rs/).